INTERNATIONAL JOURNAL OF CLIMATOLOGY
Int. J. Climatol. (2015)
Published online in Wiley Online Library
(wileyonlinelibrary.com) DOI: 10.1002/joc.4321

RMetS
Royal Meteorological Society

Influence of eastern Pacific and central Pacific El Niño events on winter climate extremes over the eastern and central United States

Liang Ning[a,b,c,d]* and Raymond S. Bradley[c]

[a] *Key Laboratory of Virtual Geographic Environment of Ministry of Education, School of Geography Science, Jiangsu Key Laboratory for Numerical Simulation of Large Scale Complex System, School of Mathematical Science, Nanjing Normal University, China*
[b] *Jiangsu Key Laboratory for Numerical Simulation of Large Scale Complex System, School of Mathematical Science, Nanjing Normal University, China*
[c] *Northeast Climate Science Center and Department of Geosciences, University of Massachusetts – Amherst, MA, USA*
[d] *Jiangsu Center for Collaborative Innovation in Geographical Information Resource Development and Application, Nanjing, China*

ABSTRACT: Different influences of the eastern-Pacific (EP) El Niño and central-Pacific (CP) El Niño on nine winter extreme indices over the eastern and central United States are examined through composite analysis of high-resolution daily maximum temperature, minimum temperature, and precipitation for the period 1950–2010. During EP El Niño winters, there are usually more warm days and warm nights, fewer frost days, cold days, and cold nights over the eastern and central United States than in winters with a CP El Niño, especially for the Ohio Valley, around the Great Lakes, and southern New England. For precipitation extremes, compared with CP El Niño, EP El Niño usually brings more extreme precipitation amounts, more days with large precipitation amounts, larger amounts of maximum consecutive 5-day total precipitation, and a shorter duration of consecutive dry days around the Great Lakes and Ohio Valley. The 500 hPa geopotential height anomalies show that wave train patterns differ when the maximum tropical sea surface heating locations are displaced. The corresponding wind field and moisture convergence anomalies are examined to analyse the mechanisms that drive the anomaly fields associated with the two types of El Niño events.

KEY WORDS EP-El Niño; CP-El Niño; winter climate extremes; teleconnection

Received 18 November 2014; Revised 23 February 2015; Accepted 25 February 2015

1. Introduction

Climate extremes have attracted increasing attention in current climate studies because of their large impacts on the economy and society (Easterling *et al.*, 2000; Meehl and Tebaldi, 2004). The Intergovernmental Panel on Climate Change (IPCC) Fifth Assessment Report (AR5) indicates that there is strong evidence that increasing global mean temperature has led to changes in temperature extremes since the mid-20th century, and increases in heavy precipitation with regional differences (Hartmann *et al.*, 2013). When using the HadEX2 data set, Donat *et al.* (2013) found widespread significant changes in temperature extremes consistent with warming since the beginning of the 20th century, and spatially heterogeneous trends in precipitation indices, with more areas with significant increasing trends in extreme precipitation amount, intensity, and frequency than areas with decreasing trends. These trends of climate extremes are consistent with previous studies on a global scale (Frich *et al.*, 2002; Alexander *et al.*, 2006) and over specific regions (e.g. Goodess *et al.*, 2005; Trenberth *et al.*, 2007; Ning and Qian, 2009; Seneviratne *et al.*, 2012).

The eastern and central United States encompasses enormous diversity in geography, climate, ecological resources, and human land use. It also includes 7 of the 21 regions established for the National Landscape Conservation Cooperative (LCC) Program and a large human population. Regional hydrology, agriculture, fisheries, and ecosystems will be increasingly compromised in the future by climate change impacts (Horton *et al.*, 2014). Consequently, the eastern and central US region poses many unique challenges for understanding, adapting to, and mitigating the effects of climate change (Ning *et al.*, 2015). Previous studies have shown that several prominent large-scale circulation modes, such as the North Atlantic oscillation (NAO; Wallace and Gutzler, 1981; Barnston and Livezey, 1987), Pacific-North American pattern (PNA; Wallace and Gutzler, 1981; Leathers *et al.*, 1991), and El Niño–Southern oscillation (ENSO; Trenberth, 1997), have strong influences on both mean climate (e.g. Rasmusson and Wallace, 1983; Ropelewski and Halpert, 1986; Hartley and Keables, 1998; Kunkel and Angel, 1999; Bradbury *et al.*, 2003; Ning *et al.*, 2012a, 2012b;

* Correspondence to: L. Ning, Department of Geosciences, University of Massachusetts – Amherst, 134 Morrill Building, Amherst, MA 01003, USA. E-mail: lning@geo.umass.edu

Ning and Bradley, 2014) and climate extremes of this region (e.g. Bradbury *et al.*, 2002; Wettestein and Mearns, 2002; Brown *et al.*, 2008; Ning and Bradley, 2015). For example, Griffiths and Bradley (2007) indicate that positive Arctic Oscillation (AO) is a good predictor of winter warm nights, while La Niña conditions usually induce more consecutive dry days in the northeastern United States.

Recent studies have revealed differences in the types of El Niño that develop. Some are located over the central tropical Pacific (CP) region and are distinct from the conventional eastern Pacific (EP) El Niño (Ashok *et al.*, 2007; Kug *et al.*, 2009). Kao and Yu (2009) applied a method combining empirical orthogonal function (EOF) analysis and linear regression on surface observations and subsurface ocean assimilation datasets to separate the two types of El Niño, and found that mechanisms triggering them are different: EP El Niño events are associated with basin-wide thermocline and surface wind variation, while CP El Niño events are more influenced by atmospheric forcing. Satellite observations suggest that the intensity of El Niño events in the central equatorial Pacific has almost doubled in the past three decades, and this is related to the increasing intensity as well as occurrence frequency of CP El Niño events since the 1990s (Lee and McPhaden, 2010). Although some studies argued that the shift in El Niño could be a part of natural variability in the tropical climate system (Ashok and Yamagata, 2009; Yeh *et al.*, 2011), model simulations indicated that projections of anthropogenic climate change are associated with an increased frequency of the CP El Niño compared to the EP El Niño, and this change is related to a flattening of the thermocline in the equatorial Pacific (Yeh *et al.*, 2009). When using the CMIP5 models to evaluate the intensity of the CP and EP types of El Niño, Kim and Yu (2012) find that the CP-to-EP ENSO intensity ratio is almost the same in the pre-industrial and historical simulations but increases in the future representative concentration pathway 4.5 (RCP4.5) scenario simulations. These results indicate that under the background of warming, the future frequency of CP El Niño events will probably increase.

EP El Niño and CP El Niño have different influences on the climate over the United States. For example, Larkin and Harrison (2005) compare the weather anomalies over the United States during the conventional El Niño and CP El Niño seasons and find positive winter temperature anomalies and precipitation anomalies during conventional El Niño conditions over the eastern United States. When examining the interdecadal modulation of the impact of ENSO on precipitation and temperature over the United States, Mo (2010) concluded that the more frequent occurrence of the CP ENSO in the recent period might explain decadal differences in the ENSO impact on the hydroclimate over the United States. Those differences include recent weakened cooling over the south and warming over the north, and a stronger influence over precipitation anomalies across the southwest, and a weaker influence over precipitation anomalies in the Ohio Valley. Liang *et al.* (2014) also found that CP El Niño and EP El Niño have opposite effects on spring soil water hydrology in the Mississippi River Basin, with higher soil water levels than average during EP El Niño years and lower soil water levels than average during CP El Niño years. Yu *et al.* (2012) used both observations and numerical model results to investigate the different impacts on US winter temperatures from EP El Niño and CP El Niño due to different wave train responses in the atmosphere to the sea surface temperature (SST) anomalies associated with the two types of El Niño, and found that EP El Niño affects winter temperature primarily over the Great Lakes, northeastern, and Southwestern United States, whereas the impacts from CP El Niño are primarily over the northwestern and southeastern United States.

However, those previous studies mainly focused on mean winter temperature and precipitation, and the influences of EP and CP El Niño on winter climate extremes, were not fully addressed. In this study, the different influences of EP and CP El Niño on nine climate extreme indices over eastern and central United States, and their corresponding mechanisms, are analysed. The analysis will improve our understanding of the dynamics of climate extreme events, and help reduce the uncertainties of predictions of El Niño impacts on regional climate extremes, which are highly relevant to a wide range of inter-disciplinary interests, such as regional water resources, ecosystems, and environment.

2. Data and methodology

2.1. Data

The study area covers the entire eastern and central United States (25°–50°N and 100°–68°W; c.f. Figure 1). The high-resolution (1/8°) observed daily maximum temperature, minimum temperature, and precipitation data used in this analysis are for the period 1950–2010. This data set developed by Maurer *et al.* (2002) covers the whole United States, and it is based on the observed data from National Oceanic and Atmospheric Administration (NOAA) Cooperative Observation stations.

The winter climate extreme indices are calculated for December, January, February, and March (DJFM), as in previous studies (Kunkel and Angel, 1999; Bradbury *et al.*, 2003) because winter conditions usually persist through March over the northeastern United States, especially over the New England area. The monthly gridded 1000–500 hPa geopotential height, *u*- and *v*-components of the wind, omega field, and specific humidity fields with a resolution of 2.5° × 2.5° for period 1950–2010 are used in the composite analysis [from the National Centers for Environmental Prediction (NCEP) reanalysis data sets (Kistler *et al.*, 2001)].

2.2. Indices of climate extremes

The nine indices of climate extremes used in this study are listed in Table 1. These indices are taken from the dictionary of European Climate Assessment and Dataset

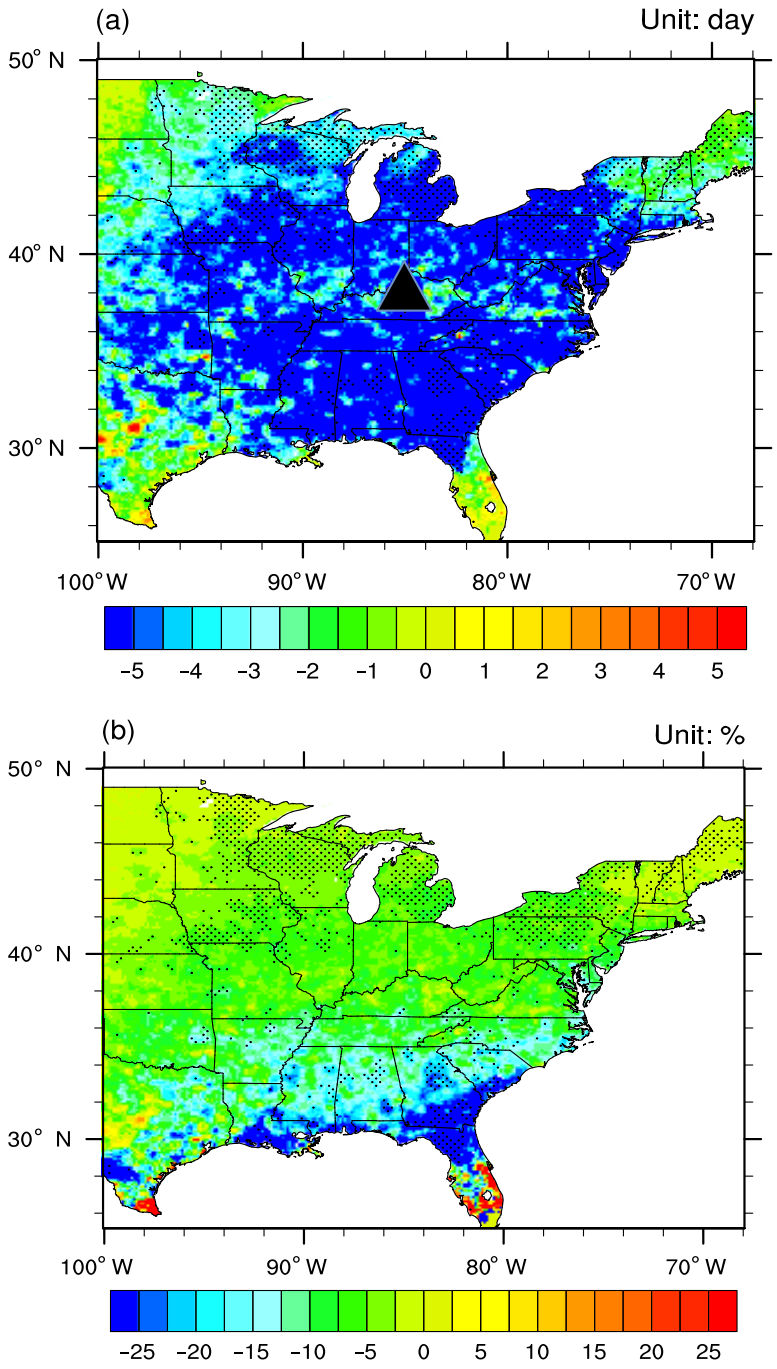

Figure 1. The differences of the seasonal number of frost days defined as EP El Niño winters – CP El Niño winters (a, unit: day) and the corresponding percentages (b, unit: %). The stippled indicate the changes significant at the 10% level. The triangle indicates the location used in the probability distribution function (PDF) calculation in Figure 12.

(ECA&D), which has been commonly used in previous studies about climate extremes (Frich *et al.*, 2002; Meehl and Tebaldi, 2004; Alexander *et al.*, 2006). Precise definitions of the full list of indices are available at the ECA&D website http://eca.knmi.nl/indicesextremes/indicesdictionary.php. These nine indices cover a wide range of inter-disciplinary interests and concerns about the potential impacts of climate change. For example, the total number of frost days (Fd) is important in future agricultural decision making. Numbers of cold days have large impacts on winter electricity consumption. The number of days with daily precipitation larger than 10 mm (R10mm) is an important factor when driving hydrological models.

3. Results

3.1. Differences

To examine the different influences from EP El Niño and CP El Niño on the regional climate extremes, composite analysis is applied to the nine winter climate extreme indices. There are usually three different definitions of EP

Table 1. The definitions and units of the nine climate extreme indices used in this study.

	Index	Definition	Unit
Temperature indices	Fd	Frost days: number of days with daily minimum temperature lower than 0 °C	Days
	Tx90p	Warm days: number of days with maximum temperature higher than 90th percentile of daily maximum temperature	Days
	Tx10p	Cold days: number of days with maximum temperature lower than 10th percentile of daily maximum temperature	Days
	Tn90p	Warm nights: number of days with minimum temperature higher than 90th percentile of daily minimum temperature	Days
	Tn10p	Cold nights: number of days with minimum temperature lower than 10th percentile of daily minimum temperature	Days
Precipitation indices	R95pTOT	Total precipitation amount due to daily precipitation larger than 95th percentile of daily	mm
	Rx5day	Maximum total precipitation over five continuous days	mm
	R10mm	Number of days with daily precipitation larger than 10 mm	Days
	CDD	Maximum length of consecutive dry days	Days

Table 2. The years of major EP and CP El Niño events (adapted from Yu *et al.*, 2012).

	El Niño years
EP El Niño	1951/1952, 1969/1970, 1972/1973, 1976/1977, 1982/1983, 1986/1987, 1997/1998, 2006/2007
CP El Niño	1953/1954, 1957/1958, 1958/1959, 1963/1964, 1965/1966, 1968/1969, 1977/1978, 1987/1988, 1991/1992, 1994/1995, 2002/2003, 2004/2005, 2009/2010

El Niño and CP El Niño: (1) the El Niño Modoki index method using the second EOF mode of the monthly tropical Pacific SST anomalies as El Niño Modoki (Ashok *et al.*, 2007), (2) the EP/CP-index method using the leading EOF mode of equatorial Pacific SST anomalies with Niño1 + 2 index regression removed as CP El Niño and leading EOF mode of equatorial Pacific SST anomalies with Niño-4 index regression removed as EP El Niño (Kao and Yu, 2009), and (3) the Niño3/4 method using Niño-4 index as CP El Niño and Niño-3 index as EP El Niño (Yeh *et al.*, 2009). In this study, in order to include large sample size of EP El Niño and CP El Niño winters, we use a definition based on at least two of the three methods (Yu *et al.*, 2012) shown in Table 2. For the period 1950–2010, there are 8 EP El Niño events and 13 CP El Niño events.

Figure 1 shows the differences in the number of winter Fd between EP El Niño winters and CP El Niño winters, and corresponding percentages. Over most regions, consistent with more average temperature anomalies during EP El Niño winters (Larkin and Harrison, 2005), the differences are negative, indicating there are fewer Fd during EP El Niño winters, with the larger magnitudes over the region from the Great Lakes to about 28°N. Most of the differences are significant at the 90% level based on a Student's *t*-test (Figure 1(a)). These corresponding percentages are −5 to −10% over most parts of the region, with the largest (−25%) around 30°N (Figure 1(b)). If compared with neutral winters, which are defined as the winters with no EP or CP El Niño events, there are significantly fewer Fd over the north part of the study region during the EP El Niño winters (Figure S1(a), Supporting Information), while during CP El Niño winters, there are significantly more Fd over the southeastern United States (Figure S1(b)). This indicates that the impacts on the Fd from the two types of El Niño events are significant.

The differences in cold days (Figure 2(a)) and cold nights (Figure 2(b)) show similar results to the Fd, with the patterns shifting slightly to the south. Negative differences are located over the region south of 43°N, and there are positive differences over northern New England, and west of Lake Michigan. For cold days (Figure 2(a)), the largest differences are located in the southeastern United States, with most significant differences located over the coastal part of this region. For the differences in cold nights (Figure 2(b)), the magnitudes are usually smaller than in cold days, but only a few differences are significant. These results show that during EP El Niño winters, there are usually fewer cold days and cold nights over most of the eastern and central United States (∼−15 to 30%), but more cold days and cold nights over northern New England and west of Lake Michigan (∼10%). The reason for non-significance is discussed in Section 3.2.

For the number of winter warm days (Figure 3(a)) and warm nights (Figure 3(b)), there are positive differences over nearly the whole region. The magnitude of differences (corresponding percentages of 20–50%) is larger and more significant than the cold days and cold nights, indicating that these two indices are very sensitive to the El Niño patterns. Noticeably, for warm nights, most of the positive differences are significant at the 90% level, and this is distinct from the cold nights.

The spatial patterns of the differences in indices of daily precipitation extremes between EP El Niño winters and CP El Niño winters are more complicated. The differences in the winter amount of extreme precipitation are given in Figure 4(a). Over regions west of the Great Lakes (36°–46°N, 90°–100°W), the New England coastal region, and the southeastern United States, there are

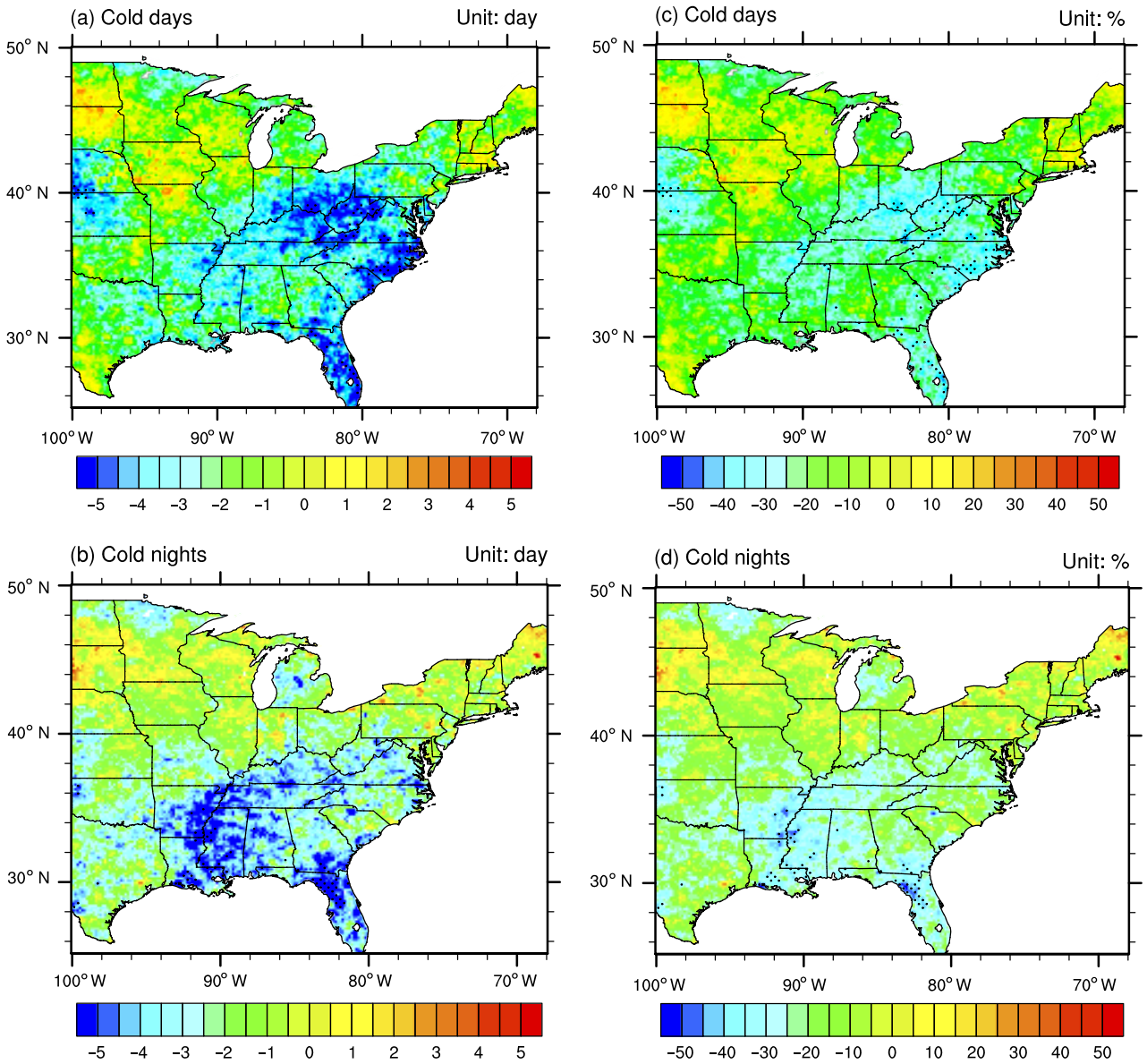

Figure 2. The differences of the seasonal number of cold days (a) and cold nights (b) defined as EP El Niño winters – CP El Niño winters (unit: day) and the corresponding percentages (c and d, unit: %).

significant positive differences with more extreme precipitation over these regions with magnitudes of 20–50 mm season^{-1} (corresponding percentages of 30–50%). In contrast, over the region from the Ohio Valley to inland New England, there are negative differences indicating less extreme precipitation with differences of −20 to −50 mm season^{-1} (corresponding percentages of −20 to −50%). This pattern is similar to the comparison of mean precipitation anomalies between EP El Niño winters and CP El Niño winters (Larkin and Harrison, 2005; Mo, 2010). Compared with neutral winters, there is significantly less extreme precipitation over the Ohio Valley and more extreme precipitation over the surrounding area during EP El Niño winters (Figure S2(a)). During CP El Niño winters, there is significantly less extreme precipitation over most of the study region, especially over the northwest, and south of the Ohio Valley (Figure S2(b)). Therefore, the impacts on extreme precipitation from the two types of El Niño events are significant.

The spatial patterns of differences of R5d (maximum consecutive 5 day total precipitation) (Figure 5(a)) and R10mm (daily precipitation totals >10 mm) (Figure 6(a)) are similar to the amount of extreme precipitation but more spatially homogeneous. For R5d (Figure 5), the positive differences over the northwest and southeast of the eastern and central United States are about 15 to 30 mm season^{-1} (corresponding percentages of 20–50%), indicating that during EP El Niño winters, the maximum consecutive 5-day total precipitation is usually larger than this during CP El Niño winters. Over the region from the Ohio Valley to inland New England, the decreases of R5d are about −15 mm season^{-1} (corresponding percentages of −20 to −30%). For R10mm (Figure 6), the region with positive differences extends to the western part of the Ohio

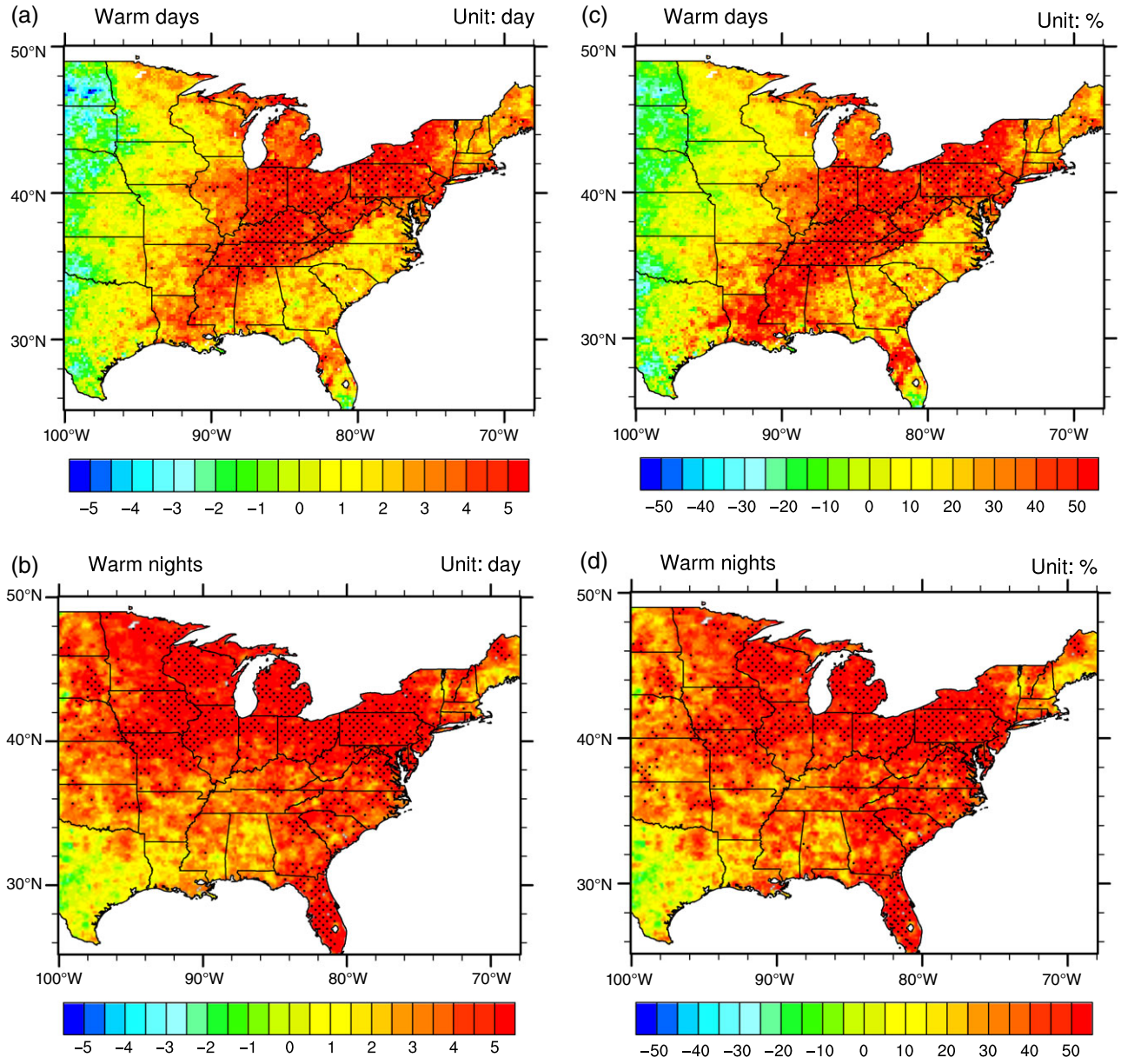

Figure 3. The differences of the seasonal number of warm days (a) and warm nights (b) defined as EP El Niño winters – CP El Niño winters (unit: day) and the corresponding percentages (c and d, unit: %).

Valley, although the magnitudes are only about 1.5 days and are not significant. Most significant increases are located west of the Great Lakes (36°–46°N, 90°–100°W) and the southeastern United States with magnitudes of 1.5–4 days (corresponding percentages of 20–50%). On the other hand, the negative differences are mainly located over the southern part of the Ohio Valley with magnitudes of 1.5 days, corresponding to −10%.

The spatial pattern of differences in the maximum length of consecutive dry days (Figure 7) is different from the previous three indices. Negative differences are located over much of the domain with magnitudes of −1 to −5 days (corresponding percentages of −10 to −30%), so during EP El Niño winters, the maximum length of consecutive dry days is usually shorter. These negative differences are significant over the region around the Great Lakes and some regions of the southeastern United States. In contrast, over the northwestern part of the domain and the New England inland region, there are positive differences of about 1.5–5 days (~20%), indicating more consecutive dry days during EP El Niño winters.

3.2. Mechanisms

Previous studies have shown that large changes in both intensity and frequency of climate extremes can result from small changes in mean climate variables (e.g. temperature and precipitation), because of the nonlinear relationships between climate means and extremes (Mearns *et al.*, 1984; Wigley, 1985; Wettestein and Mearns, 2002). Therefore, in this section, the differences of seasonal mean synoptic circulation patterns between EP El Niño winters and CP El Niño winters, which will result in changes of winter

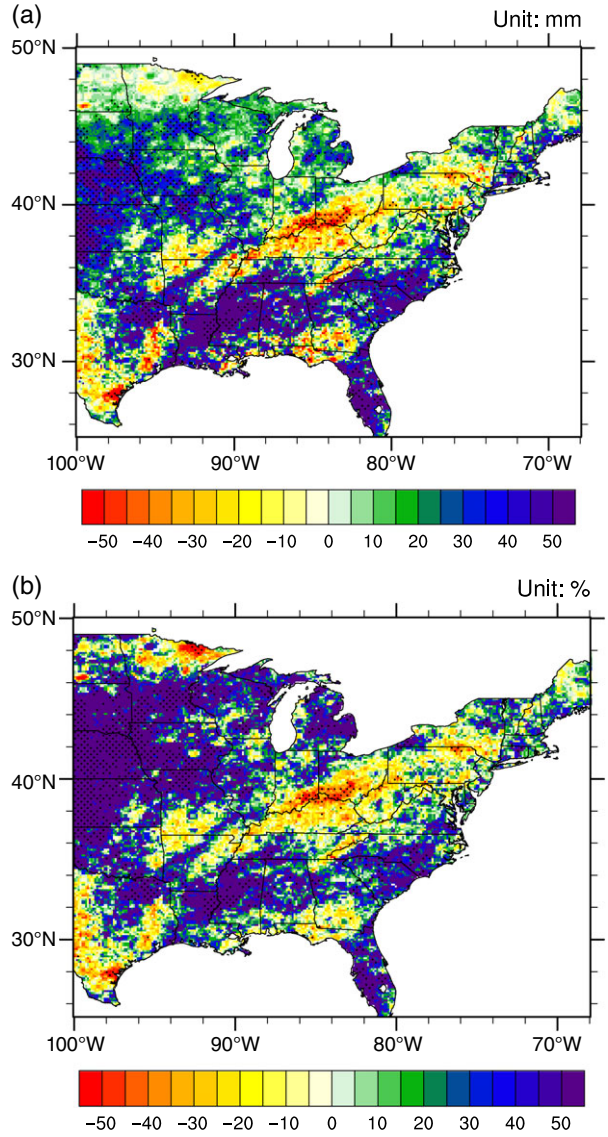

Figure 4. The differences of the seasonal amount of extreme precipitation defined as EP El Niño winters – CP El Niño winters (a, unit: mm season^{-1}) and the corresponding percentages (b, unit: %).

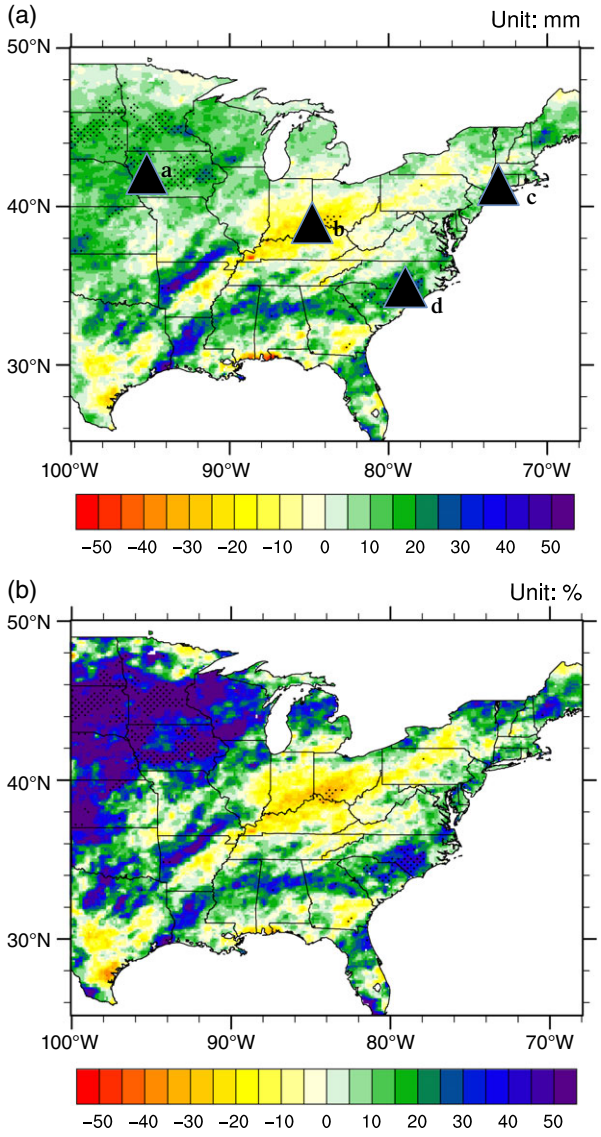

Figure 5. The differences of the seasonal amount of maximum consecutive 5-day total precipitation defined as EP El Niño winters – CP El Niño winters (a, unit: mm season^{-1}) and the corresponding percentages (b, unit: %). The triangles indicate the locations used in the CDFs calculation in Figure 13.

mean maximum and minimum temperature, and precipitation, are first compared through composite analyses. Then, the responses of daily maximum temperature, minimum temperature, and precipitation to the seasonal mean states are examined through the changes in the probability distributions.

3.2.1. Relationships with the large-scale synoptic circulation

One major mechanism by which El Niño influences the regional climate over the eastern and central United States is through the PNA (Wallace and Gutzler, 1981; Leathers *et al.*, 1991). Previous studies (Horel and Wallace, 1981; Hoskins and Karoly, 1981) have shown that the excitation of tropospheric Rossby waves by the anomalous tropical SSTs associated with ENSO is a major dynamical link between the tropics and subtropics. The climatological stationary planetary waves and associated jet streams in the northern hemisphere can influence the total Rossby wave sources, i.e. strong upper tropospheric divergence in the tropics and convergence in the subtropics, and thus can create preferred teleconnection response patterns, such as the PNA pattern (Trenberth *et al.*, 1998). Alexander *et al.* (2002) reviewed this connection in previous studies augmented by analyses of reanalysis data and coupled model experiments. They found that observational and modelling studies have now established a clear link between SST anomalies in the equatorial Pacific, north tropical Atlantic, and Indian Oceans in boreal winter and spring, and atmosphere–ocean coupling in the extratropical Pacific modifies the atmospheric circulation anomalies in the PNA region. Straus and Shukla (2000) also showed that with external forcing, the PNA pattern and its probability of occurrence are linked to the pattern of tropical Pacific SST anomalies.

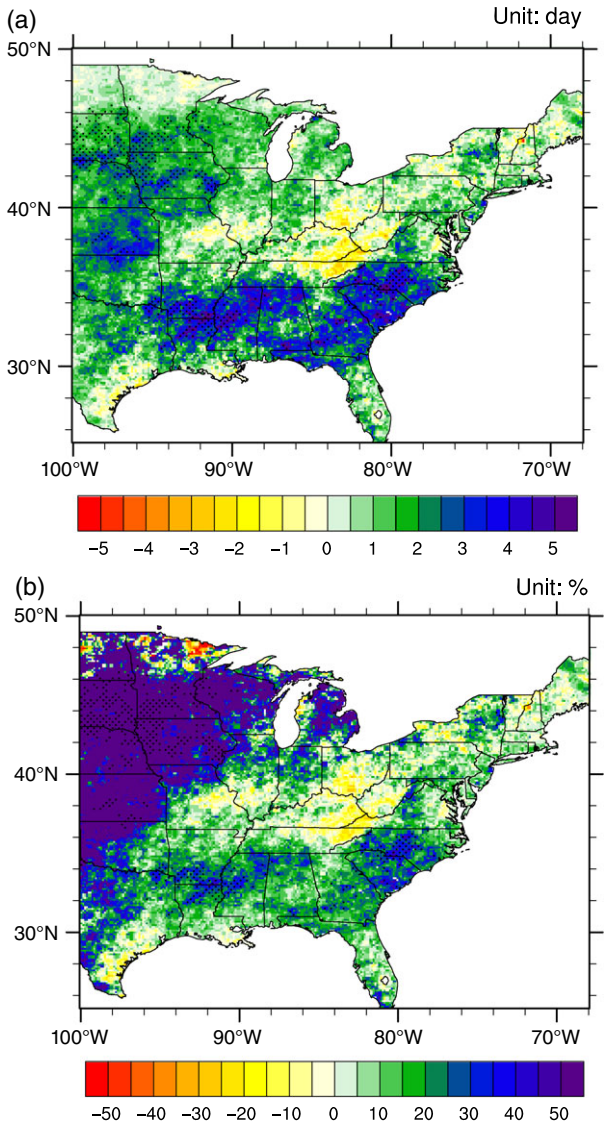

Figure 6. The differences of the seasonal number of days with daily precipitation larger than 10 mm defined as EP El Niño winters – CP El Niño winters (a, unit: day) and the corresponding percentages (b, unit: %).

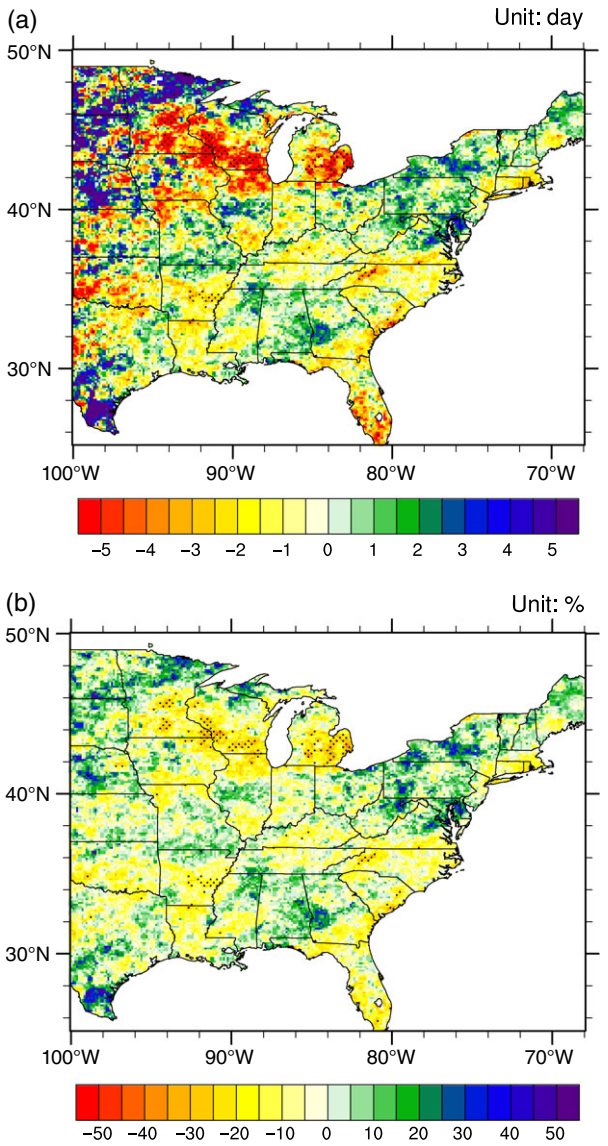

Figure 7. The differences of the seasonal maximum length of consecutive dry days defined as EP El Niño winters – CP El Niño winters (a, unit: day) and the corresponding percentages (b, unit: %).

Therefore, when the deep convective heating locations are different during the EP and CP El Niño events (Wang *et al.*, 2013), the corresponding planetary wave train patterns are also different (Zou *et al.*, 2014). To investigate this mechanism, Figure 8 compares the 500-hPa geopotential height anomalies of the ordinary high PNA winter, EP El Niño winters, and CP El Niño winters. The ordinary high PNA winters are defined as those winters with PNA indices one standard deviation higher than the long-term mean excluding the EP El Niño winters, and CP El Niño winters. For this analysis, the ordinary high PNA winters are 1952/1953, 1960/1961, 1980/1981, 1985/1986, and 2000/2001 winters. For the ordinary high PNA winters, there is a significant negative anomaly centred over the northern Pacific, a significant positive anomaly centred over northwestern North America, and a negative anomaly centred over southeastern North America (Figure 8(a)). For EP El Niño winters, the positive anomaly centre is located more towards northeastern North America, and the negative anomaly centre located over the Southeast is shifted towards the Southwest (Figure 8(b)). For the CP El Niño winters, the positive anomaly centre and negative anomaly centre over North America extends further to the east (Figure 8(c)). These differences in 500 hPa geopotential height anomaly patterns between EP El Niño winters and CP El Niño winters were also found by Yu *et al.* (2012). Compared with ordinary high PNA winters, the positions of the geopotential height anomaly centres over North America during EP El Niño winters and CP El Niño winters are dramatically different. This indicates that when there is external forcing from the tropical ocean in the form of El Niño, the PNA zonal wave train pattern over North America changes to a more meridional wave train pattern. When the thermal heating is located over the eastern tropical Pacific, the wave train pattern over North America is northeast–southwest

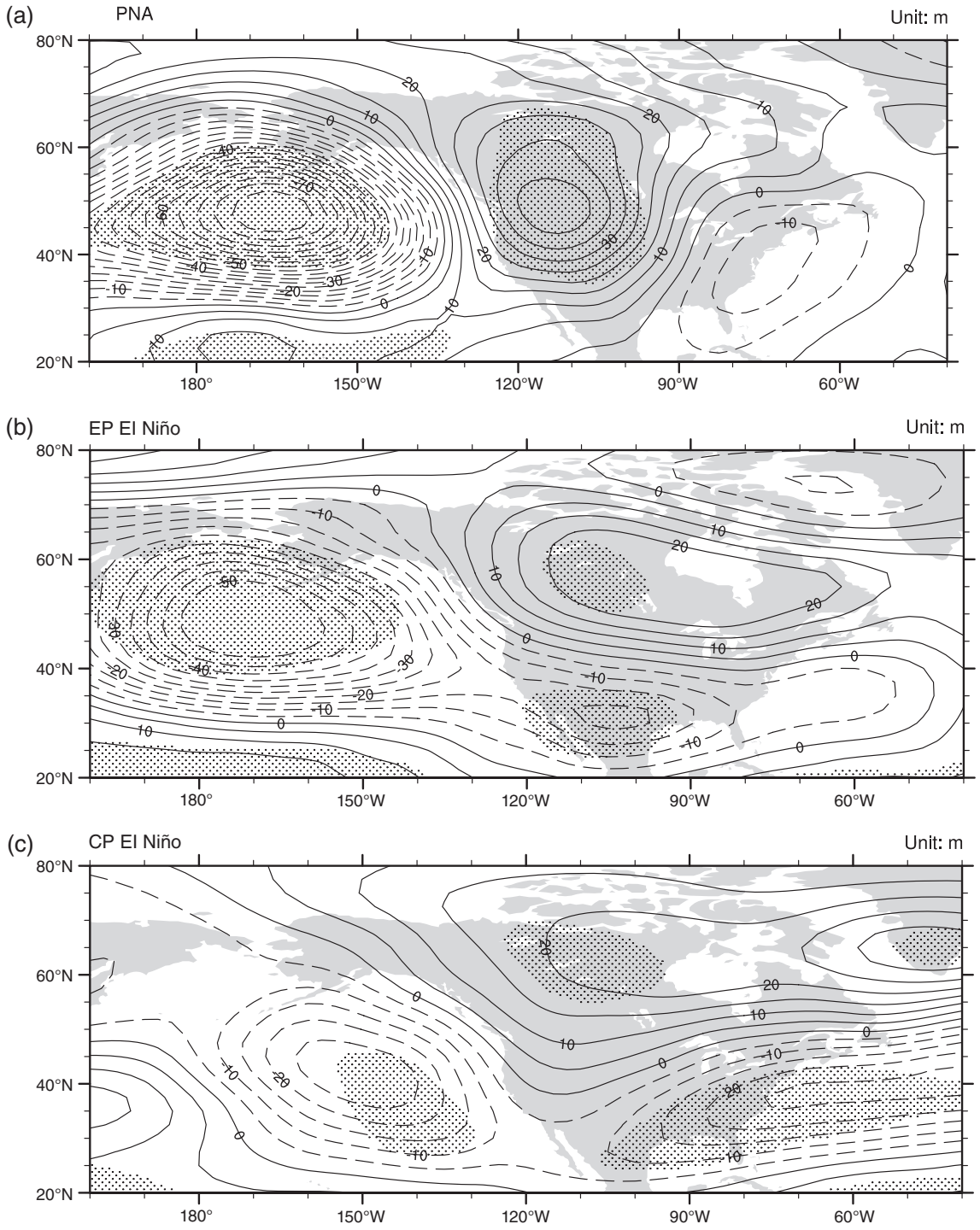

Figure 8. The comparison of 500 hPa geopotential height anomalies of ordinary high PNA winters (a), EP El Niño winters (b), and CP El Niño winters (c) (unit: m). The stippled indicate the changes significant at the 5% level.

(positive–negative geopotential height anomaly) pattern. On the other hand, when the heating is located over the central tropical Pacific, the corresponding wave train pattern is northwest–southeast.

These different geopotential height anomaly patterns during EP El Niño winters and CP El Niño winters will induce different circulation patterns. Taking 850 hPa level as an example, during EP El Niño winters, the positive geopotential height anomaly centred over northeastern North America induces an anti-cyclonic circulation pattern, which brings northerly wind anomalies over New England, southerly wind anomalies to the west of the Great Lakes, and easterly anomalies over the rest of the eastern and central United States. (Figure 9(a)). During CP El Niño winters, the circulation pattern over the eastern and central United States is mainly cyclonic, controlled by the negative geopotential height anomaly centre over southeastern North America, and this cyclonic circulation

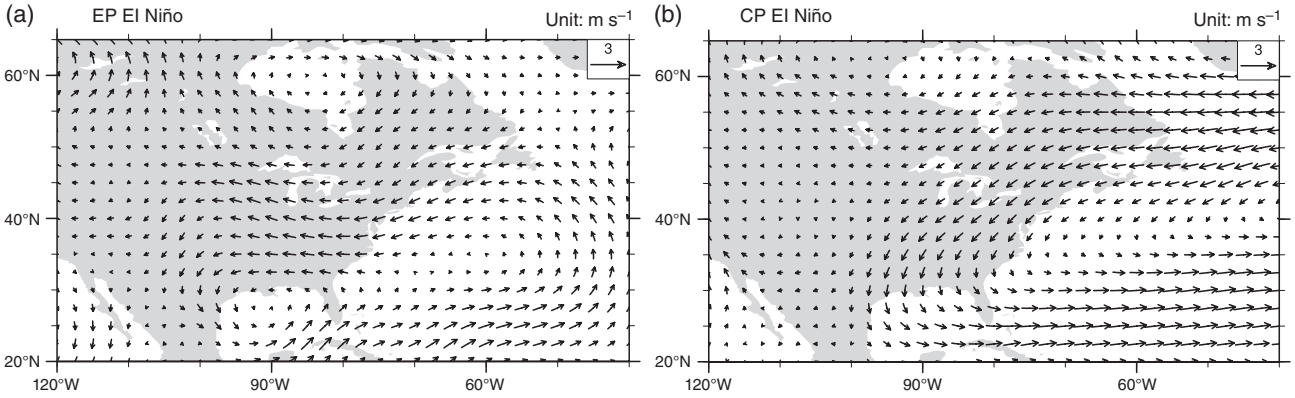

Figure 9. The comparison of 850 hPa wind field anomalies between EP El Niño winters (a) and CP El Niño winters (b) (unit: m s^{-1}).

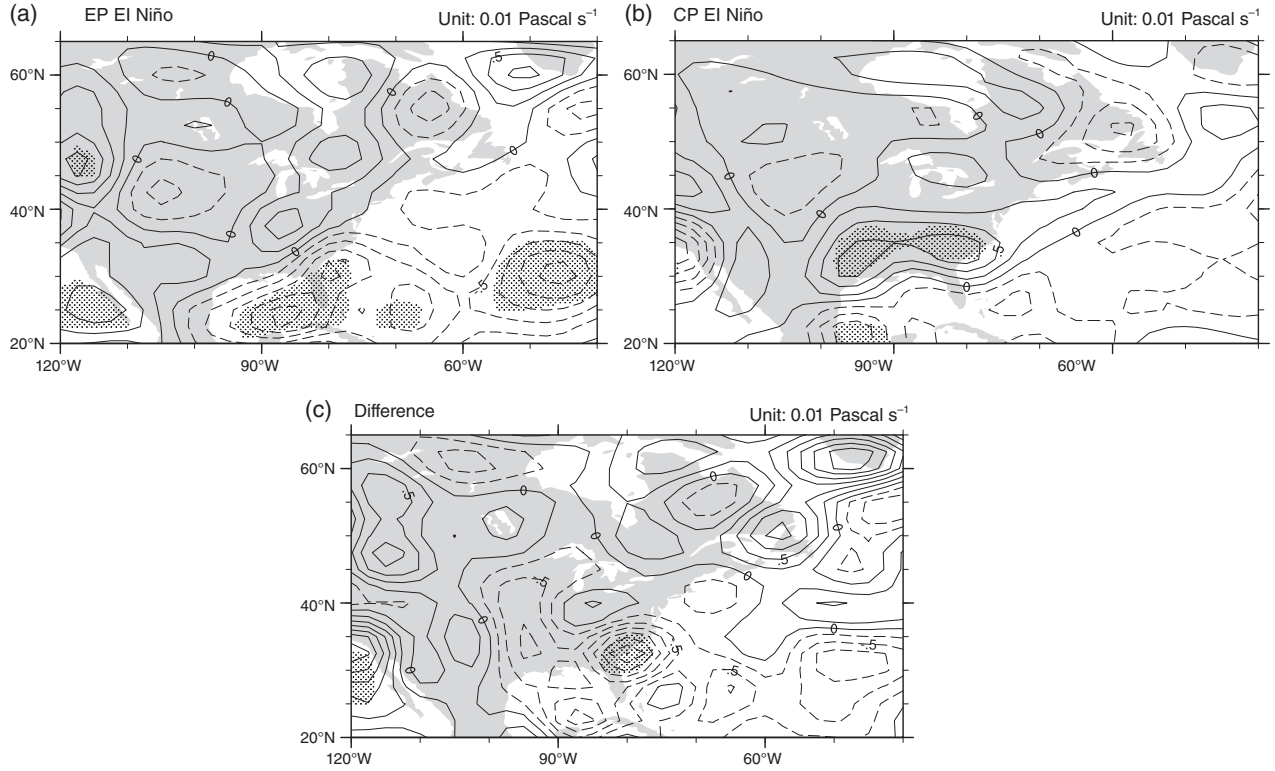

Figure 10. The comparison of low-level (1000–500 hPa) omega anomalies between EP El Niño winters (a), and CP El Niño winters (b), and their differences (EP–CP; c) (unit: 10^{-2} Pascal s^{-1}). Negative contours are dashed.

induces mainly northern wind anomalies over most part of the eastern and central United States. (Figure 9(b)). The temperature advection associated with the wind anomalies brings lower winter average temperature over most parts of the eastern and central United States during CP El Niño winters compared to EP El Niño winters.

To investigate the mechanisms influencing the differences of precipitation extremes, two aspects that are highly relevant to the precipitation processes are analysed here: the vertical velocity and water vapour transport. Mo (2010) showed that the divergence field over the eastern United States is different during EP El Niño and CP El Niño events due to the different locations of tropical ocean thermal heating and corresponding shifts of the North American jet stream. To investigate this mechanism in detail, the low-level (1000–500 hPa) average omega anomalies measuring the vertical velocity during EP El Niño winters show that there are three centres over the study region: one negative anomaly centred west of the Great Lakes, one positive anomaly centred over the Ohio Valley, and another negative anomaly centred over the southeastern United States, and only the latter negative anomalies are statistically significant (Figure 10(a)). Negative omega anomalies indicate strong upward movement, which induces precipitation, whereas positive omega anomalies indicate strong downward movement, which tends to inhibit precipitation. For CP El Niño winters, there is mainly a significant positive omega anomaly centre over the region south of Ohio Valley (Figure 10(b)). When comparing these two patterns, their differences show a positive

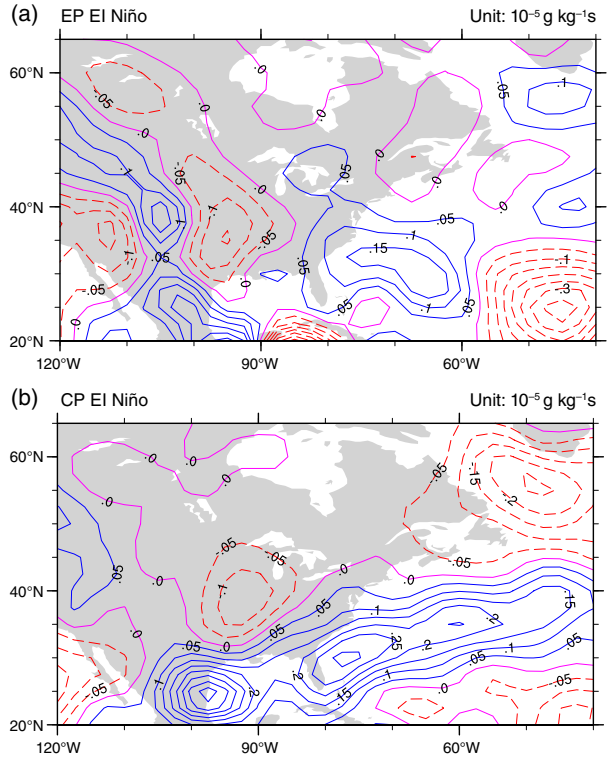

Figure 11. The comparison of low-level (1000–500 hPa) moisture convergence anomalies between EP El Niño winters (a) and CP El Niño winters (b) (unit: 10^{-5} g kg^{-1} s).

anomaly centred over the Ohio Valley and negative anomalies around the Ohio valley over the southeastern United States, although only the latter negative anomalies are statistically different (Figure 10(c)). This difference pattern may partly explain why there is less precipitation over the Ohio Valley, but more precipitation over the surrounding region during EP El Niño winters.

When taking humidity into consideration, the low-level (1000–500 hPa) moisture convergence anomaly pattern during EP El Niño winters shows that there is moisture convergence (negative values) over the region west of the Great Lakes from the west, and moisture divergence (positive values) over the region from the east coast to the Great Lakes (Figure 11(a)). However, during CP El Niño winters (Figure 11(b)), the moisture convergence slightly shifts to the east with weaker magnitude, and moisture divergence extend to the Gulf of Mexico with larger magnitudes. Therefore, during EP El Niño winters, there is more moisture over the region west of the Great Lakes and south of the Appalachian Mountains, but less moisture over the Ohio Valley.

3.2.2. *Responses of daily variables*

The probability distributions of daily maximum and minimum temperatures (Figure 12) during EP El Niño winters and CP El Niño winters are compared to examine the responses of the daily variables to the differences of mean synoptic circulation patterns discussed in the previous section. Because the differences of the temperature extremes are fairly spatially homogeneous (Figures 1–3), one location in the centre of study region was selected to calculate the probability distributions of daily maximum and minimum temperature. The location is shown as a triangle in Figure 2(a). For daily precipitation, four locations (Figure 5(a)) were selected to represent the four major regions with different responses to EP El Niño winters and CP El Niño winters.

From Figure 12, it can be seen that during the EP El Niño winters, the probability distributions of daily maximum temperature and minimum temperature shift to the right compared with those during the CP El Niño winters. The average values of daily maximum temperature and minimum temperature during the EP El Niño winters are more than 1° higher than the average values during the CP El Niño winters. The widths of the probability distributions of daily maximum temperature, defined as the distances between 75 and 25% threshold values, are close under the two El Niño conditions, indicating that the influences mainly shift the probability distributions. For the daily minimum temperature, the width during EP El Niño winters is smaller than CP El Niño winters, indicating the influences from EP El Niño not only shift the probability distribution to the right side but also cluster the daily minimum temperature values in the middle. Therefore, the differences of probability distributions can be used to explain that there are more warm extremes and less cold extremes during the EP El Niño winters. When applying Student's *t*-tests to both daily maximum temperature and minimum temperature probability distributions during EP El Niño winters and CP El Niño winters, their differences are statistically significant ($p < 0.01$). One interesting point is that on the left tails, the distributions of the EP El Niño winters are slightly higher than those of the CP El Niño winters, and this explains why the differences in cold days and cold nights are not as significant as warm days and warm nights (Figures 2 and 3). However, for the Fd, because they are defined using a certain value (0 °C) that is located over the right half of the daily minimum temperature probability distributions and covers more than half of the distribution domain, this slight overlap (<−20 °C) does not influence Fd. Consequently, the differences in the number of Fd between EP El Niño winters and CP El Niño winters are more significant than the cold days and cold nights (Figure 1). Moreover, the average of daily maximum temperature during neutral winters is 8.31 °C, and this is lower than the average of EP El Niño winters (8.45 °C), and significantly higher than the average of CP El Niño winters (7.39 °C) based on Student's *t*-test ($p < 0.05$). For daily minimum temperature, the average during neutral winters is −3.2 °C, and this significantly lower than the average of EP El Niño winters (−2.65 °C) based on Student's *t*-test ($p < 0.05$), and significantly higher than the average of CP El Niño winters (−3.63 °C) based on Student's *t*-test ($p < 0.05$).

Similar analysis of daily precipitation is shown in Figure 13. To clearly show the details of the probabilities over the large daily precipitation values, cumulative distribution functions (CDFs) rather than probability

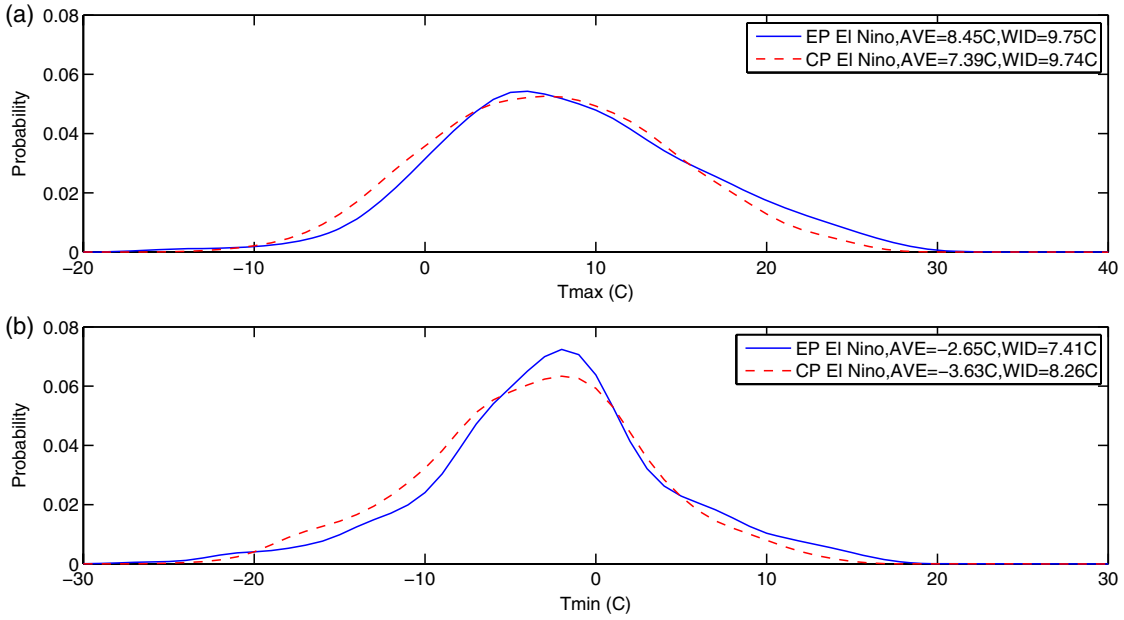

Figure 12. The comparisons of probability distributions of daily maximum temperature (a) and daily minimum temperature (b) between EP El Niño winters (blue solid lines) and CP El Niño winters (red dashed lines).

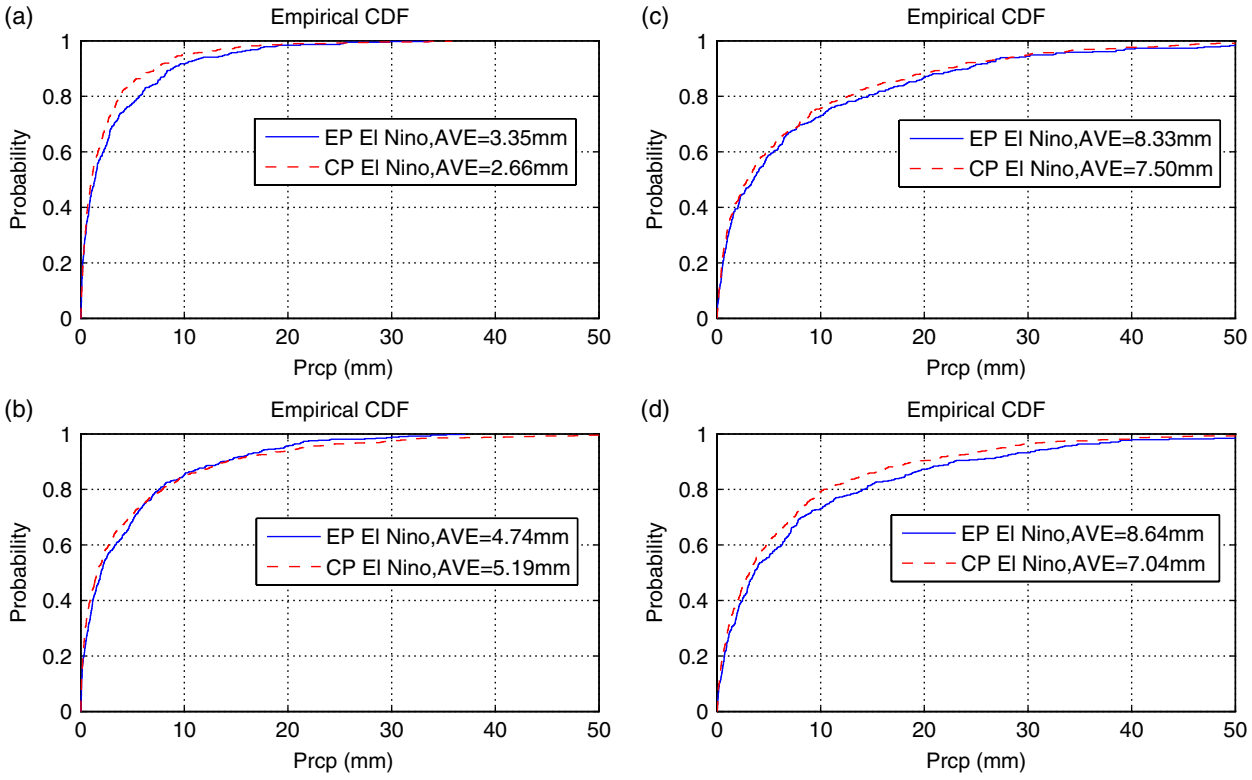

Figure 13. The comparisons of cumulative distributions of daily precipitation over the four locations between EP El Niño winters (blue solid lines) and CP El Niño winters (red dashed lines).

distributions are shown here, and all the days without precipitation are removed. For the region west of the Great Lakes, the CDF during EP El Niño winters shifts to the right side with larger average values (Figure 13(a)), indicating the there are higher possibilities of extreme precipitation events. For the Ohio Valley, the CDF during EP El Niño winters slightly shifts to the left side with smaller average values (Figure 13(b)), indicating lower possibilities of extreme precipitation events. For the coastal region over New England and the southeastern United States, both the CDFs during EP El Niño winters shift to the right side, with larger average values (Figure 13(c) and (d)), but the difference over the southeastern United States is more obvious. These differences

of the CDFs during EP El Niño winters and CP El Niño winters show that the response of daily precipitation values to the synoptic circulation patterns leads to more precipitation extremes over the region west of the Great Lakes, the coastal region of New England, and the southeastern United States, and fewer precipitation extremes over the Ohio Valley, although these CDFs are not statistically different at $p = 0.05$ level when applied to a Kolmogorov–Smirnov test.

4. Conclusion

The different influences of two El Niño circulation types (eastern and central Pacific El Niño) on nine winter climate extreme indices of high societal relevance to the eastern and central United States were investigated, together with their corresponding physical mechanisms. Composite analyses show that over most parts of the eastern and central United States, during EP El Niño winters, there are usually more warm days and warm nights, and fewer Fd, cold days, and cold nights than during CP El Niño winters. Moreover, during EP El Niño winters, there are more precipitation extremes (i.e. greater extreme precipitation amounts, more days with large precipitation amounts, and larger maximum consecutive 5-day total precipitation amounts) over the region west of the Great Lakes, the New England coast, and the southeastern United States, but fewer precipitation extremes over the Ohio Valley. For the maximum length of consecutive dry days, the relationships are the opposite.

Because the locations of tropical ocean heating are different during the two El Niño conditions, the corresponding wave train patterns on the 500 hPa geopotential height field are different. During the EP El Niño winters, the wave train pattern is a northeast-to-southwest positive–negative geopotential height anomaly, while during CP El Niño winters, the wave train pattern is northwest-to-southeast. Both of these two patterns are distinct from the zonal pattern during ordinary high PNA winters. These wave train patterns induce cold temperature advection over most parts of the eastern and central United States during CP El Niño conditions, but warm temperature advection over large parts of the region during EP El Niño conditions. Therefore, the probability distributions of daily maximum temperature and minimum temperature significantly shift to the right sides during CP El Niño winters, indicating higher probabilities of warm extremes and lower probabilities of cold extremes.

A comparison of low-level moisture convergence and omega anomalies can be used to explain the positive precipitation anomalies over the region west of the Great Lakes, the New England coast, and the southeastern United States, and negative precipitation anomalies over the Ohio Valley. In these regions with positive precipitation anomalies, the CDFs of daily precipitation values shift to the right sides, indicating higher probabilities of precipitation extremes, while in areas with negative precipitation anomalies the CDF shift slightly to the left side, indicating lower probabilities of precipitation extremes.

These findings of different influences on the regional climate extremes from EP and CP El Niño events, and their corresponding mechanisms, contribute to better understanding of climate extremes over the eastern and central United States. When applied to future general circulation model (GCM) simulations, these relationships can help improve the projections of regional climate extremes and corresponding mitigations of the socio-economic impacts from future climate changes.

Acknowledgements

This research is jointly supported by the US Department of the Interior's Northeast Climate Science Center, under USGS funding G12AC00001, the Strategic and Special Frontier Project of Science and Technology of the Chinese Academy of Sciences (grant no. XDA05080800), and The Priority Academic Development Program of Jiangsu Higher Education Institutions (grant no. 164320H101). We want to thank Henry F. Diaz for fruitful discussions. Edwin P. Maurer (Santa Clara University) kindly provided the observational data. The NCEP grid data were obtained from The National Centers for Environmental Prediction (NCEP). We acknowledge high-performance computing support from Yellowstone (ark:/85065/d7wd3xhc) provided by NCAR's Computational and Information Systems Laboratory, sponsored by the National Science Foundation.

Supporting Information

The following supporting information is available as part of the online article:

Figure S1. The comparison of the seasonal number of frost days between EP El Niño winters and neutral winters (a, unit: day), and between CP El Niño winters and neutral winters (b, unit: day). The stippled indicate the changes significant at the 10% level.

Figure S2. The comparison of the seasonal extreme precipitation amounts between EP El Niño winters and neutral winters (a, unit: mm), and between CP El Niño winters and neutral winters (b, unit: mm). The stippled indicate the changes significant at the 10% level.

References

Alexander MA, Bladé I, Newman M, Lanzante JR, Lau N-C, Scott JD. 2002. The atmospheric bridge: the influence of ENSO teleconnections on air-sea interaction over the global oceans. *J. Clim.* **15**: 2205–2229.

Alexander LV, Zhang X, Peterson TC, Caesar J, Gleason B, Klein Tank AMG, Haylock M, Collins D, Trewin B, Rahimzadeh F, Tagipour A, Rupa Kumar K, Revadekar J, Griffiths G, Vincent L, Stephenson DB, Burn J, Aguilar E, Brunet M, Taylor M, New M, Zhai P, Rusticucci M, Vazquez-Aguirre JL. 2006. Global observed changes in daily climate extremes of temperature and precipitation. *J. Geophys. Res.* **111**: D05109, doi: 10.1029/2005JD006290.

Ashok K, Yamagata T. 2009. The El Nino with a difference. *Nature* **461**: 481–484.

Ashok K, Behera SK, Rao SA, Weng H, Yamagata T. 2007. El Niño Modoki and its possible teleconnection. *J. Geophys. Res.* **112**: C11007, doi: 10.1029/2006JC003798.

Barnston AG, Livezey RE. 1987. Classification, seasonality, and persistence of low-frequency atmospheric circulation patterns. *Mon. Weather Rev.* **115**: 1083–1126.

Bradbury JA, Dingman SL, Keim BD. 2002. New England drought and relations with larger scale atmospheric circulation patterns. *J. Am. Water Resour. Assoc.* **38**: 1287–1299.

Bradbury JA, Keim BD, Wake CP. 2003. The influence of regional storm tracking and teleconnections on winter precipitation in the Northeastern United States. *Ann. Assoc. Am. Geogr.* **93**: 544–556.

Brown SJ, Caesar J, Ferro CAT. 2008. Global changes in extreme daily temperature since 1950. *J. Geophys. Res.* **113**: D05115, doi: 10.1029/2006JD008091.

Donat MG, Alexander LV, Yang H, Durre I, Vose R, Dunn RJH, Willett KM, Aguilar E, Brunet M, Caesar J, Hewitson B, Jack C, Klein Tank AMG, Kruger AC, Marengo J, Peterson TC, Renom M, Oria Rojas C, Rusticucci M, Salinger J, Elrayah AS, Sekele SS, Srivastava AK, Trewin B, Villarroel C, Vincent LA, Zhai P, Zhang X, Kitching S. 2013. Updated analysis of temperature and precipitation extreme indices since the beginning of the twentieth century: the HadEX2 dataset. *J. Geophys. Res. Atmos.* **118**: 2098–2118, doi: 10.1002/jgrd.50150.

Easterling DR, Meehl GA, Parmesan C, Changnon SA, Karl TR, Mearns LO. 2000. Climate extremes: observations, modeling, and impacts. *Science* **289**: 2068–2074.

Frich P, Alexander LV, Della-Marta P, Gleason B, Haylock M. 2002. Observed coherent changes in climatic extremes during the second half of the twentieth century. *Clim. Res.* **19**: 193–212.

Goodess CM and STARDEX consortium. 2005. STARDEX final report. http://www.cru.uea.ac.uk/projects/stardex/reports/STARDEX_FINAL_REPORT.pdf (accessed 4 July 2013).

Griffiths ML, Bradley RS. 2007. Variations of twentieth-century temperature and precipitation extreme indicators in the northeast United States. *J. Clim.* **20**: 5401–5417.

Hartley S, Keables MJ. 1998. Synoptic associations of winter climate and snowfall variability in New England, USA, 1950–1992. *Int. J. Climatol.* **18**: 281–298.

Hartmann DL, Klein Tank AMG, Rusticucci M, Alexander LV, Brönnimann S, Charabi Y, Dentener FJ, Dlugokencky EJ, Easterling DR, Kaplan A, Soden BJ, Thorne PW, Wild M, Zhai PM. 2013. Observations: atmosphere and surface. In *Climate Change 2013: The Physical Science Basis. Contribution of Working Group I to the Fifth Assessment Report of the Intergovernmental Panel on Climate Change*, Stocker TF, Qin D, Plattner G-K, Tignor M, Allen SK, Boschung J, Nauels A, Xia Y, Bex V, Midgley PM (eds). Cambridge University Press: Cambridge, UK and New York, NY.

Horel JD, Wallace JM. 1981. Planetary-scale atmospheric phenomena associated with the Southern Oscillation. *Mon. Weather Rev.* **109**: 813–829.

Horton R, Yohe G, Easterling W, Kates R, Ruth M, Sussman E, Whelchel A, Wolfe D, Lipschultz F. 2014. Northeast (Chapter 16). In *Climate Change Impacts in the United States: The Third National Climate Assessment*, Melillo JM, Richmond TC, Yohe GW (eds). U.S. Global Change Research Program: Washington, DC, 371–395, doi: 10.7930/J0SF2T3P.

Hoskins BJ, Karoly DJ. 1981. The steady linear response of a spherical atmosphere to thermal and orographic forcing. *J. Atmos. Sci.* **38**: 1179–1196.

Kao H-Y, Yu J-Y. 2009. Contrasting eastern-Pacific and central-Pacific types of ENSO. *J. Clim.* **22**: 615–632.

Kim ST, Yu J-Y. 2012. The two types of ENSO in CMIP5 models. *Geophys. Res. Lett.* **39**: L11704, doi: 10.1029/2012GL052006.

Kistler R, Kalnay E, Collins W, Saha S, White G, Woollen J, Chelliah M, Ebisuzaki W, Kanamitsu M, Kousky V, van den Dool H, Jenne R, Fiorino M. 2001. The NCEP-NCAR 50-year reanalysis: monthly means CD-ROM and documentation. *Bull. Am. Meteorol. Soc.* **82**: 247–267.

Kug J-S, Jin F-F, An S-I. 2009. Two types of El Niño events: cold tongue El Niño and warm pool El Niño. *J. Clim.* **22**: 1499–1515.

Kunkel KE, Angel JR. 1999. Relationship of ENSO to snowfall and related cyclone activity in the contiguous United States. *J. Geophys. Res.* **104**(D16): 19425–19434.

Larkin NK, Harrison DE. 2005. Global seasonal temperature and precipitation anomalies during El Niño autumn and winter. *Geophys. Res. Lett.* **32**: L16705, doi: 10.1029/2005GL022860.

Leathers DJ, Yarnal B, Palecki MA. 1991. The Pacific/North American teleconnection pattern and United States climate. Part I: regional temperature and precipitation associations. *J. Clim.* **4**: 517–528.

Lee T, McPhaden MJ. 2010. Increasing intensity of El Niño in the central-equatorial Pacific. *Geophys. Res. Lett.* **37**: L14603, doi: 10.1029/2010GL044007.

Liang Y-C, Lo M-H, Yu J-Y. 2014. Asymmetric responses of land hydroclimatology to two types of El Niño in the Mississippi River Basin. *Geophys. Res. Lett.* **41**: 582–588, doi: 10.1002/2013GL058828.

Maurer EP, Wood AW, Adam JC, Lettenmaier DP, Nijssen B. 2002. A long-term hydrologically-based data set of land surface fluxes and states for the conterminous United States. *J. Clim.* **15**(22): 3237–3251.

Mearns LO, Katz RW, Schneider SH. 1984. Extreme high-temperature events: changes in their probabilities with changes in mean temperature. *J. Clim. Appl. Meteorol.* **23**: 1601–1613.

Meehl GA, Tebaldi C. 2004. More intense, more frequent, and longer lasting heat waves in the 21st century. *Science* **305**: 994–997.

Mo K. 2010. Interdecadal modulation of the impact of ENSO on precipitation and temperature over the United States. *J. Clim.* **23**: 3639–3656.

Ning L, Bradley RS. 2014. Winter precipitation variability and corresponding teleconnections over the northeastern United States. *J. Geophys. Res. Atmos.* **119**: 7931–7945, doi: 10.1002/2014JD021591.

Ning L, Bradley RS. 2015. Winter climate extremes over the northeastern United States and southeastern Canada and teleconnections with large-scale modes of climate variability. *J. Clim.* **28**: 2475–2493, doi: 10.1175/JCLI-D-13-00750.1.

Ning L, Qian Y. 2009. Interdecadal change of extreme precipitation over South China and its mechanism. *Adv. Atmos. Sci.* **26**: 109–118.

Ning L, Mann ME, Crane R, Wagener T. 2012a. Probabilistic projections of climate change for the mid-Atlantic region of the United States – validation of precipitation downscaling during the historical era. *J. Clim.* **25**: 509–526.

Ning L, Mann ME, Crane R, Wagener T, Najjar RG Jr, Singh R. 2012b. Probabilistic projections of anthropogenic climate change impacts on precipitation for the mid-Atlantic region of the United States. *J. Clim.* **25**: 5273–5291.

Ning L, Riddle EE, Bradley RS. 2015. Projected changes in climate extremes over the northeastern United States. *J. Clim.* **28**, doi: 10.1175/JCLI-D-14-00150.1.

Rasmusson EM, Wallace JM. 1983. Meteorological aspects of the El Niño/Southern Oscillation. *Science* **222**: 1195–1202.

Ropelewski CF, Halpert MS. 1986. North American precipitation and temperature patterns associated with the El Niño/Southern Oscillation (ENSO). *Mon. Weather Rev.* **114**: 2352–2361.

Seneviratne SI, Nicholls N, Easterling D, Goodess CM, Kanae S, Kossin J, Luo Y, Marengo J, McInnes K, Rahimi M, Reichstein M, Sorteberg A, Vera C, Zhang X. 2012. Changes in climate extremes and their impacts on the natural physical environment. In *Managing the Risks of Extreme Events and Disasters to Advance Climate Change Adaptation*, A Special Report of Working Groups I and II of the Intergovernmental Panel on Climate Change (IPCC), Field CB, Barros V, Stocker TF, Qin D, Dokken DJ, Ebi KL, Mastrandrea MD, Mach KJ, Plattner G-K, Allen SK, Tignor M, Midgley PM (eds). Cambridge University Press: Cambridge, UK and New York, NY, 109–230.

Straus DM, Shukla J. 2000. Distinguishing between the SST-forced variability and internal variability in mid latitudes: analysis of observations and GCM simulations. *Q. J. R. Meteorol. Soc.* **126**: 2323–2350.

Trenberth KE. 1997. The definition of El Niño. *Bull. Am. Meteorol. Soc.* **78**: 2771–2777.

Trenberth KE, Branstator GW, Karoly D, Kumar A, Lau N-C, Ropelewski C. 1998. Progress during TOGA in understanding and modeling global teleconnections associated with tropical sea surface temperatures. *J. Geophys. Res.* **103**: 14291–14324.

Trenberth KE, Jones PD, Ambenje P, Bojariu R, Easterling D, Klein Tank A, Parker D, Rahimzadeh F, Renwick JA, Rusticucci M, Soden B, Zhai P. 2007. Observations: Surface and Atmospheric Climate Change. In *Climate Change 2007: The Physical Science Basis*. Contribution of Working Group I to the Fourth Assessment Report of the Intergovernmental Panel on Climate Change, Solomon S, Qin D, Manning M, Chen Z, Marquis M, Averyt KB, Tignor M, Miller HL (eds). Cambridge University Press: Cambridge, UK and New York, NY.

Wallace JM, Gutzler DS. 1981. Teleconnections in the geopotential height field during the Northern Hemisphere winter. *Mon. Weather Rev.* **109**: 784–812.

Wang C, Deser C, Yu J-Y, DiNezio P, Clement A. 2013. El Niño and Southern Oscillation (ENSO): a review. In *Coral Reefs of the Eastern Pacific*, Glynn P, Manzello D, Enochs I (eds). Springer-Verlag: New York, NY (in press).

Wettestein JJ, Mearns LO. 2002. The influence of North Atlantic – Arctic Oscillation on mean, variance, and extremes of temperature in the northeastern United States and Canada. *J. Clim.* **15**: 3586–3600.
Wigley TML. 1985. Impact of extreme events. *Nature* **316**: 106–107.
Yeh S-W, Kug J-S, Dewitte B, Kwon M-H, Kirtman BP, Jin F-F. 2009. El Niño in a changing climate. *Nature* **461**: 511–514.
Yeh S-W, Kirtman BP, Kug J-S, Park W, Latif M. 2011. Natural variability of the central Pacific El Niño event on multi-centennial timescales. *Geophys. Res. Lett.* **38**: L02704, doi: 10.1029/2010GL045886.
Yu J-Y, Zou Y, Kim ST, Lee T. 2012. The changing impact of El Niño on US winter temperatures. *Geophys. Res. Lett.* **39**: L15702, doi: 10.1029/2012GL052483.
Zou Y, Yu J-Y, Lee T, Lu M-M, Kim ST. 2014. CMIP5 model simulations of the impacts of the two types of El Niño on the U.S. winter temperature. *J. Geophys. Res. Atmos.* **119**: 3076–3092, doi: 10.1002/2013JD021064.

